

## Research Article

Cecilie B. Devantier and Niels Daugbjerg\*

# Intraspecific variation in growth rates of *Rhodomonas marina* (Cryptophyceae) under different temperatures and salinities conditions: a comparative study of six Arctic and one temperate strain

<https://doi.org/10.1515/bot-2024-0080>

Received February 24, 2025; accepted September 4, 2025;  
published online September 23, 2025

**Abstract:** Marine and freshwater cryptophytes are highly valued for their nutritional content and are commonly used as live feed for copepods in aquaculture. Few studies have examined the impact of temperature and salinity on growth rates of several cryptophyte strains isolated from the same water sample. This study presents the first multi-strain autecological analysis of an Arctic marine cryptophyte species, using six strains of *Rhodomonas marina* and one temperate strain to explore intraspecific variation. Phylogenetic inference based on ITS revealed a close relationship among all *R. marina* strains (99.6–100 % sequence similarity). The autecological study used batch cultures, examining growth rates at three salinities and five temperatures in one-parameter experiments. One Arctic strain and the temperate strain were also examined at 20.1 and 23.2 °C. All strains grew over a wide range of temperatures and salinities, classifying them as eurythermal and euryhaline. However, the temperate strain exhibited higher phenotypic plasticity concerning temperature, while the Arctic strains showed greater plasticity regarding salinity. Thus, this study identified the presence of intraspecific variation within a confined Arctic marine water mass, highlighting an economic potential when selecting the fastest-growing isolates for biomass production and commercial applications.

**Keywords:** Arctic nanoflagellate; autecology; growth rates; resilience; *Rhodomonas*

## 1 Introduction

Marine primary producers, including the cryptophyte *Rhodomonas marina* (P. A. Dangeard) Lemmermann emend. Daugbjerg *et al.* are directly influenced by changes in physical (e.g., temperature, light regime, water column stability) and chemical (e.g., salinity, nutrients, pH) variables. Due to the short doubling time of phytoplankton communities, they can therefore be used as indicators of ecosystem perturbation and ultimately changes in ecosystem services. In a geological perspective the earth's climate has always changed in natural cycles but in the last 200 years, the carbon dioxide concentration has increased significantly and most of this increase has occurred since the 1970s. Earth's climate is expected to change further (IPCC 2023; Stocker *et al.* 2013) and one of the likely consequences is alterations in the seasonal and yearly composition of phytoplankton communities (Thomalla *et al.* 2023; Winder and Sommer 2012; Yamaguchi *et al.* 2022). According to Barton *et al.* (2016) these climate change driven alterations may be considerable. Possible shifts in phytoplankton can be characterized either by modeling whole communities (Henson *et al.* 2021) or by conducting autecological studies of growth rates in single species (e.g., Pančić *et al.* 2015).

For temperature alone numerous studies have shown that an increase in sea surface temperatures (SST) altered the community composition of phytoplankton (e.g., Beaugrand *et al.* 2010, 2015; Behrenfeld *et al.* 2006; Bopp *et al.* 2005; Comeau *et al.* 2011; Daufresne *et al.* 2009; Edwards and Richardson 2004; Li *et al.* 2009) and therefore ecosystem functioning (e.g., primary production) within the area (Winder and Sommer 2012). Additionally, changes in salinity

\*Corresponding author: Niels Daugbjerg, Marine Biological Section, Department of Biology, University of Copenhagen, Universitetsparken 4, DK-2100 Copenhagen Ø, Denmark, E-mail: n.daugbjerg@bio.ku.dk. <https://orcid.org/0000-0002-0397-3073>

Cecilie B. Devantier, Marine Biological Section, Department of Biology, University of Copenhagen, Universitetsparken 4, DK-2100 Copenhagen Ø, Denmark, E-mail: cebd@dhigroup.com

of Arctic marine ecosystems due to sea ice melt, river runoff and precipitation may also favor a shift in community structure and changes in size groups (e.g., Guinder and Molinero 2013; Li et al. 2009). Such changes may be detrimental as phytoplankton play a vital role as climate regulators, in biogeochemical cycles (Winder and Sommer 2012) and globally they account for up to half of the total primary production (Behrenfeld et al. 2006; Guinder and Molinero 2013; Käse and Geuer 2018).

For this study, six strains of *R. marina* were isolated from a single water sample collected at Disko Bay, western Greenland (see Daugbjerg and Devantier (2024) for the biogeographical distribution of *R. marina*). Given the significance of temperature (Beaugrand et al. 2010; Salles and Mercado 2020; Winder et al. 2012) and salinity (Li et al. 2009) on phytoplankton growth as also recognized by the IPPC, this study aimed to elucidate their effect on the growth of multiple strains from a single microalgal species derived from the same population. This would allow interpretation of intraspecific variation and thus levels of resilience for this species towards future climate changes in temperature and salinity. For more accurate modeling a better understanding of growth rate variation even within single species may improve the projections. Consequently, a series of autecological experiments were conducted. Our hypothesis for the temperature experiments was that growth rates would be highest at temperatures corresponding to Arctic summer SST, which in Disko Bay (western Greenland) average around 5 °C, and lower at higher experimental temperatures. For the salinity experiments, we expected that the growth rates of all Arctic strains would remain consistent across the entire salinity range tested, indicating no intraspecific variation. For the Arctic isolates such a result would represent an euryhaline organism being in this case physiologically capable of handling salinity fluctuations due to seasonal sea ice melt and river runoff. To further explore intraspecific variation but across geographical regions, the autecology of a single temperate isolate available of *R. marina* from Kattegat (Denmark) was also studied. This strain was expected to grow slower at lower temperatures and faster than the Arctic strains at higher temperatures. With respect to the salinity experiment it was expected to grow faster at the highest salinity treatments. The genetic similarity and thus identity of the seven strains of *R. marina* was confirmed by sequence determination of the highly variable internal transcribed spacers 1 and 2 (ITS 1 and 2).

To the best of our knowledge, only a few other studies have explored the resilience of marine microalgal populations to future climate changes (e.g., Kremp et al. 2012; Pančić et al. 2015). However, the result of this study may also be of interest to industry as cryptophytes have gained great

attention due to their profile and considerable amounts of essential biochemical compounds, e.g., polyunsaturated fatty acids, phytosterols, proteins, carotenoids, phycobiliproteins and polysaccharides (Abidizadegan et al. 2021). These compounds are not only important for human and animal nutrition, cosmetics, and beauty products industry (Rizwan et al. 2018), but have also shown to be of utmost importance for production of secondary grazers in aquatic food webs (Peltomaa et al. 2018) and as feed for copepods in the aquaculture industry (Vu et al. 2016). Despite a relatively low growth rate for most cryptophytes (<0.8 divisions per day) (Abidizadegan et al. 2021) they are still considered having a great potential in biomedical and pharmaceutical applications (Vilchis 2022). However, reports on growth rates have rarely explored the presence of intraspecific (strain specific) variation between multiple isolates from a single water sample. Identifying intraspecific variation, with some strains growing significantly faster than others, allows for the selection and further characterization of these strains for valuable biochemical compounds.

## 2 Materials and methods

### 2.1 Cultures

Six strains of *Rhodomonas marina* were established into clonal cultures from a single integrated (0–20 m) and well mixed net plankton sample collected in Disko Bay, western Greenland (July 2018) at 69° 11.112' N 53° 30.995' W. Here the surface temperature at 0.8 m was 5.0 °C and declined to 1.3 °C at 20 m (data not shown). The salinity in the surface water was 31.8 and increased to 33.1 at 20 m. From July 2018 and onwards all strains were grown in L1 medium (Guillard and Hargraves 1993) and kept at 4 °C under a light:dark cycle of 16:8 h. Light was provided by LED light panels (Philips 33 W) at 40–50 µmol photons m<sup>-2</sup> s<sup>-1</sup>. The temperate strain was collected in Kattegat, Denmark (56° 11' N 12° 04' E) (April 1990) and established as a clonal culture. The Danish strain was also grown in L1 medium under a light:dark cycle of 16:8 h but kept at 15 °C. Light was provided by LED light panels (Philips 33 W) at 30–50 µmol photons m<sup>-2</sup> s<sup>-1</sup>.

### 2.2 DNA extraction and amplification of internal transcribed spacers (ITS) 1 and 2

A volume of 11 ml from seven recently inoculated strains of *R. marina* were transferred to 15 ml Falcon tubes. Cell pelleting was done by centrifugation at 1174g for 10 min at 4 °C. Pellets were transferred into 1.5-ml Eppendorf tubes

and kept frozen at  $-18^{\circ}\text{C}$  for a few days until extraction of total genomic DNA. For this the PowerPlant Pro DNA isolation kit (Mo Bio Laboratories Inc., Carlsbad, CA, USA) was used following the manufacturer's recommendations. Extracted DNA was used as template for PCR amplifications of ITS using the forward primer 'ITS1' and the reverse primer 'ITS4' (White et al. 1990). The 5× Hot FIREPol Blend Master Mix (Solis BioDyne) was used to amplify this DNA fragment. The PCR temperature profile for amplification of ITS consisted of one initial cycle of denaturation at  $95^{\circ}\text{C}$  for 12 min, then 35 cycles each consisting of denaturation at  $95^{\circ}\text{C}$  for 30 s, annealing at  $54^{\circ}\text{C}$  for 30 s and extension at  $72^{\circ}\text{C}$  for 30 s. A final extension step at  $72^{\circ}\text{C}$  lasted 6 min. Length of amplified products were confirmed by electrophoresis using an agarose gel (final concentration 1.5%). GelRed was used to stain PCR products, and these were visualized in a gel documentation XR System (BioRad, Hercules, CA, USA). For purification of PCR products, the Nucleofast 96 PCR kit from Macherey-Nagel (GmbH & Co KG, Düren, Germany) was applied following the recommendations of the manufacturer. The service provided by Macrogen was used to determine ITS sequences (including the 5.8S rDNA gene) in both directions. Amplification primers were also used for this step.

### 2.3 Alignment and phylogenetic analysis

To infer the phylogeny of the *R. marina* strains the nucleotide sequences of ITS (including 5.8S rDNA) were added to a data matrix comprising a few congeners retrieved from GenBank (i.e., *Rhodomonas salina*, *Rhodomonas maculata* and *Rhodomonas lens*). The data matrix comprised a total of 11 *Rhodomonas* strains and two ITS sequences of *Rhodomonas nottbecki* were used as outgroup taxa. This matrix included 886 bp (including introduced gaps) and was analyzed using Bayesian Analysis (BA) and Maximum Likelihood (ML). MrBayes (ver. 3.2.6, Ronquist and Huelsenbeck 2003) was set to run for 10 million generations, and a single tree was sampled for every 1000th generation. A conservative estimate of the burn-in value was obtained by plotting the  $-\text{Ln}$  score as a function of generations. The burn-in occurred after 501,000 generations, which left 9,500 trees for a majority rule consensus tree. Posterior probabilities (PP) provided statistical support for the branching pattern. jModeltest (ver. 2.1.3, Darriba et al. 2012) was used to find the best model for ML. Here the GTR-I-G model was suggested, and the settings from this model were used as input parameters for PhyML (Guindon et al. 2010) bootstrap analyses with 1,000 replications. This analysis was run on the Montpellier

bioinformatics platform and bootstrap support (BS) values were later mapped onto the tree topology obtained from BA.

### 2.4 Autecological experiments

Triplicate experiments were performed in Nunc flasks ( $75\text{ cm}^2$ ) and as batch cultures containing 50 ml of L1 media. All experiments had a start concentration of approximately 800 cells  $\text{ml}^{-1}$ . Experiments were conducted in 24-liter glass tanks containing demineralized water. A cooling system, controlled by a custom-made relay, ensured exact control of the pre-set experimental temperatures by switching on/off the cooling of the water, while a heating element provided elevated temperatures in experiments  $>15^{\circ}\text{C}$ . The water was circulated using an aquarium pump (see Daugbjerg et al. 2024, Supplementary document S1 for more details). Following experimental setup, an acclimation period of two days was initiated. Sub-samples were taken with approximately 48 h in between by initially rotating the Nunc flasks to ensure even distributions of cells. This was followed by pipetting 1,175  $\mu\text{l}$  from each triplicate experiment into 1.5-ml glass vials. The flasks were rotated randomly when returned to the glass tanks. Experiments lasted 10–20 days depending on the growth rates of individual experiments. The autecological studies were conducted as one-parameter temperature (Experiment 1) or salinity (Experiment 2) treatments as a function of time. Experiment 1 used temperatures at 1.4, 3.8, 6.7, 9.9, 13.7, 15.9  $^{\circ}\text{C}$  (all strains), and two strains (S11 and K-0435) were grown at two additional temperatures (20.1 and 23.2  $^{\circ}\text{C}$ ). The Arctic strain used for further examination at higher temperatures was randomly chosen. Temperature fluctuations around the preset values were  $\leq 0.4^{\circ}\text{C}$  (Supplementary Figure S1). All temperature experiments were conducted at salinity 31. Salinity studies included treatments at 5 and 15 kept at  $6.6 \pm 0.1^{\circ}\text{C}$  and 31 kept at  $6.7 \pm 0.2^{\circ}\text{C}$  (Supplementary Figure S2). The irradiance range was 98–110  $\mu\text{mol photons m}^{-2} \text{s}^{-1}$  and the light:dark cycle was 16:8 h. The fluorescence of Chl *a* was measured using a Trilogy fluorometer equipped with the blue module (Trilogy, Turner Designs Instruments, Sunnyvale, CA, USA). Due to a linear correlation between Chl *a* fluorescence and cells  $\text{ml}^{-1}$ , when grown at the same irradiance, a standard curve was made for each separate experiment to convert fluorometric measurements into cell abundances (data not shown). pH measurements were taken at the beginning, middle and end of the experimental periods (Supplementary Figures S3–S4). Due to photosynthesis pH increased towards the end of the experiments and cell abundances likely limited by high pH values (about 10) were excluded prior to estimation of growth rates.

## 2.5 Estimation of cell abundances based on light microscopy

Following fluorescence measurements, the volume of replicate experiments labeled A (1,175  $\mu$ l) was transferred to 1.5-ml Eppendorf tubes containing 25  $\mu$ l Lugol's iodine ( $\approx 2\%$  final conc.) for fixation. Before estimations of cell abundances using Sedgewick Rafter Cell Counters, samples were vortexed to ensure that cells did not stick to the sides of the Eppendorf tubes. Cells were counted in an Olympus microscope (BH-2) at 100 $\times$  magnification using a phase contrast objective and followed the suggestions of the IOC Manuals and Guides (LeGresley and McDermott 2010).

## 2.6 Estimation of growth rates

All growth rates were calculated using Equation (1).

$$\mu = (\ln(N_2) - \ln(N_1)) / (t_2 - t_1) \quad (1)$$

where  $N_2$  and  $N_1$  are the number of cells at time  $t_2$  and  $t_1$ , respectively (Wood et al. 2005). Growth rates ( $\mu$ ) were calculated from the exponential growth phase and thus represent the maximum growth rate.

## 2.7 Statistical analyses

The effects of treatments (salinity and temperature) were tested with simple linear regression ( $X$  = treatment,  $Y$  = growth rate). Shapiro-Wilk tests were performed to test for normality (data not shown). One-way ANOVA with Tukey *post hoc* tests were used to test for significant differences among strains and treatments, respectively. The significance level ( $\alpha$ ) was  $p = 0.05$ . All statistical analyses and graphs (including Supplementary Figures S1–S4) were made with GraphPad Prism (ver. 9).

# 3 Results

## 3.1 Molecular phylogeny

DNA fragments characterized by a high sequence variability have previously been used for identification at the taxonomic level of populations and/or species (e.g., Binzer et al. 2019). The internal transcribed spacer regions of the nuclear ribosomal cistron represent one such DNA fragment. Here it was used to infer the phylogeny between both congeners and

conspecifics and thus to support strain identification of *R. marina* from Greenland and Denmark. As shown in Figure 1, the S-strains from Disko Bay and K-0435 from Kattegat formed a highly supported monophyletic clade (PP = 1, BS = 100 %). The branch lengths were very short indicating very similar or identical sequences strongly arguing for them belonging to the same species. However, it was noted that strain K-0332 identified as *Rhodomonas* cf. *baltica* formed a sister taxon to two of the Arctic strains (S8 and S18). This calls upon reexamination of the identity of K-0332. The freshwater species *R. lens* originally described from the Austrian Alps (Lunz) and ponds in the Böhmerwald (located in central Europe) (Pascher 1913) formed a sister taxon to the *R. marina* clade (PP = 1.0 and BS = 97 %). The earliest branching lineage consisted of the marine species *R. salina*, and *R. maculata* and their relationship was highly supported (PP = 1.0, BS = 100 %).

## 3.2 Sequence similarity

Estimating the percentage sequence similarity for all pairwise comparisons of the Arctic isolates (S-strains in Figure 1) revealed values ranging between 99.6 and 100 % (data not shown). In a similar pair-wise comparison between the Danish strain (K-0435) and each of the Arctic strains the sequence similarity ranged between 99.7 and 99.9 %.

## 3.3 Autecological experiments

To evaluate the impact of temperature and salinity on growth rates of *R. marina* one-parameter experiments were conducted on seven strains. Hence, growth rates were used as a proxy to assess intraspecific variation within Disko Bay and between two climate regions (Arctic versus temperate). Fluctuations within each of the preset temperatures (Experiment 1) and the temperature used for the salinity experiment (Experiment 2) were negligible (Supplementary Figures S1–S2). All treatments at the preset temperatures in Experiment 1 were significantly different (data not shown). Also, the salinity in each of the three salinity experiments remained constant during the experimental period. pH appeared to be growth limiting when surpassing a value of ca. 10. Therefore, cell abundances used for calculations of growth rates were omitted when clearly limited by pH (Supplementary Figures S3–S4).

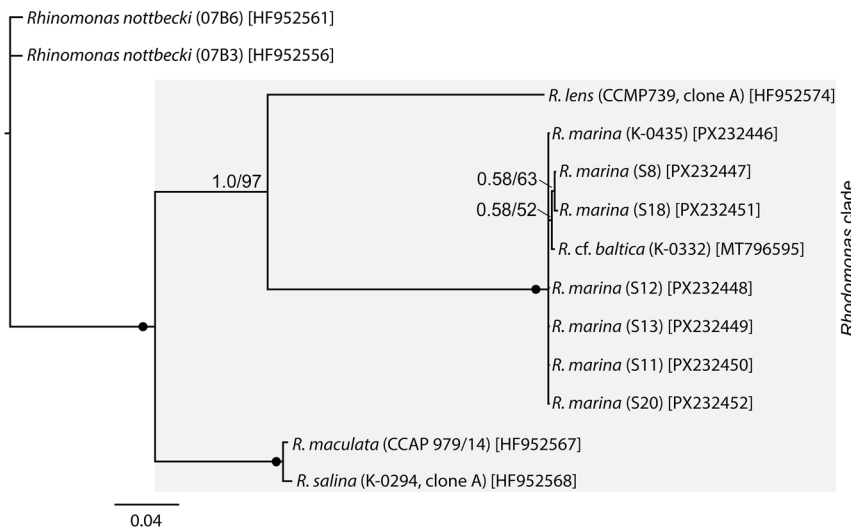


**Figure 1:** Phylogeny of *Rhodomonas* spp. based on internal transcribed spacers 1 and 2 (including 5.8S rDNA). The two sequences of *Rhinomonas nottbecki* were used as outgroup taxa. The tree topology shown was based on Bayesian analysis and the robustness of clades was evaluated from posterior probabilities and bootstrap replications from maximum likelihood, respectively. The resulting support values were written at internodes. Maximum support values (PP = 1 and bootstrap support = 100 %) were shown by filled circles and otherwise only PP  $\geq$  0.5 and bootstrap support  $\geq$  50 % were included. Strain numbers are in parentheses and GenBank accession numbers in square brackets. Branch lengths are proportional to the number of character changes.

### 3.4 Experiment 1: impact of temperature on growth rates

Based on estimates of growth rates, the Arctic strains, and the temperate strain of *R. marina* generally grew better with increasing temperatures ( $p \leq 0.0003$ ), sorted by strain in Figure 2A–G and by temperature in Figure 2H–O. However, the temperature at which these strains reached an optimum growth rate differed. For strain S12 this was reached at 6.7 °C, for strain S20 at 9.9 °C, for strains S8, S13 and S18 at 13.7 °C and for strain S11 at 20.1 °C. At higher temperatures, the growth rate was the same for strains S8, S12 and S13 or dropped significantly for strains S11, S18 and S20. It should be noted that only one Arctic strain (S11) was grown at 20.1 and 23.3 °C. A large degree of intraspecific variation was observed, and this was particularly evident for growth rates at temperatures between 3.8 and 15.6 °C (Figure 2I–M). Growth rates obtained at a temperature of 1.4 °C were more similar among the Arctic strains (Figure 2H). The overall lowest average growth rate was 0.10  $d^{-1}$  for S11 at 3.8 °C (Figure 2B) and the overall highest average growth rate was 0.99  $d^{-1}$  for S18 at 13.7 °C (Figure 2E). The variation between the lowest and highest growth rates and their percentage differences are shown in Table 1. Among the six Arctic strains the percentage difference in growth rates varied between 20 and 104.8 %. As mentioned above, the Arctic strain S11 was also grown at 20.1 and 23.2 °C (Figure 2B). The growth rate at 20.1 °C was the highest recorded for this strain

(0.75  $d^{-1}$ ) and growth ceased at 23.3 °C. Therefore, the lethal temperature for its proliferation was between these values, differing by 2.2 °C.

The temperate strain (K-0435) included showed the same general growth pattern as seen for the Arctic strains as division rates increased with increasing temperatures from 1.4 to 20.1 °C whereafter it dropped significantly at 23.2 °C (Figure 2G). The drop from 0.76  $d^{-1}$  at 20.1 °C to 0.3  $d^{-1}$  at 23.2 °C equaled a decrease of 60.5 %. The optimum temperature for growth for K-0435 was similar to the Arctic strain S11 (Figure 2B). However, K-0435 grew at 23.2 °C, which S11 did not. Interestingly, K-0435 also grew at the coldest temperature but with a significantly lower growth rate compared to four of the six Arctic strains (Figure 2H).

### 3.5 Experiment 2: impact of salinity on growth rates

Experiments with salinity 5 and 15 were conducted at  $6.6 \pm 0.1$  °C and salinity 31 at  $6.7 \pm 0.2$  °C. Hence the salinity experiment used temperatures close to summer SST in the natural environment for the Arctic strains. All seven strains (including K-0435 from temperate waters) grew at the salinities tested and their growth rates were sorted by strain in Figure 3A–G and by salinity in Figure 3H–J. The percentage difference between the lowest and highest growth rate comparing all salinity treatments ranged between 34 and

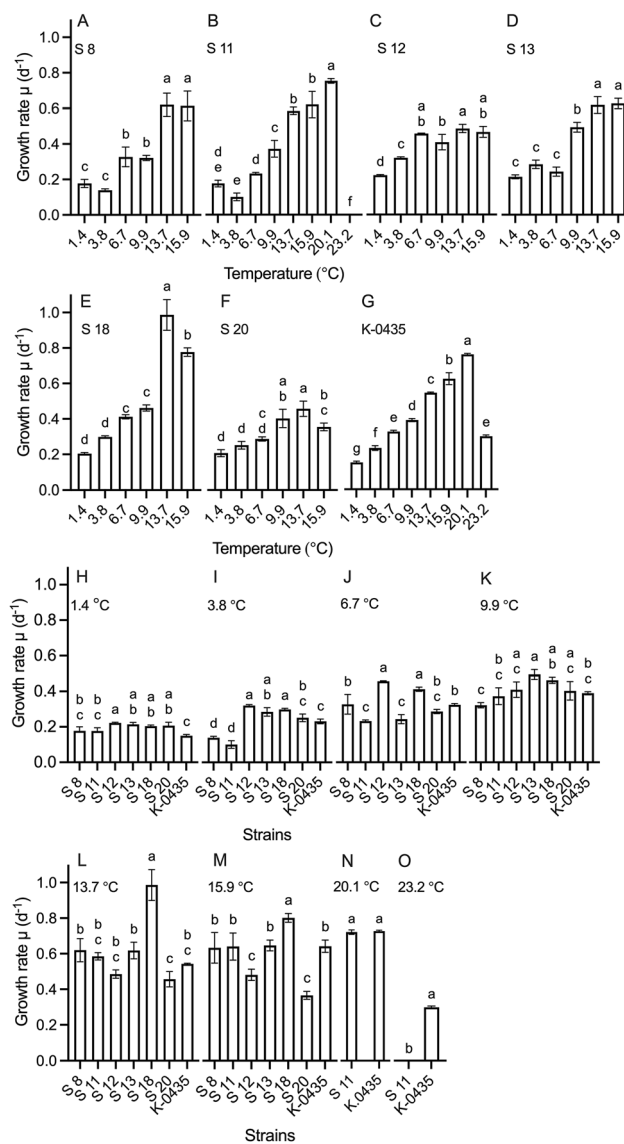


**Figure 2:** Growth rates ( $\mu \text{ day}^{-1}$ ) as a function of temperatures ranging from 1.4 to 15.9 °C (six treatments) for seven strains of *Rhodomonas marina*. Two additional temperature treatments were conducted at 20.1 and 23.2 °C for strains S11 and K-0435 (B and G, respectively). All autecological experiments were conducted as batch cultures at a salinity of 31. (A–G) Growth rates sorted by strain numbers. (H–O) Growth rates sorted by temperatures. Identical lower-case letters show non-significant differences based on Tukey (HSD) post hoc tests.

66.7 % (Table 2). Changes in salinities did not appear to affect the growth rates of *R. marina* as significantly as changes in temperature, as less intraspecific variation was observed (Figure 3H–J). No single strain was characterized by having either the highest or lowest growth rate at any salinity tested (Figure 3H–J). Rather two strains (S12 and S18) shared a significantly higher growth rate in the experiment with a salinity of 31 (Figure 3J) and three strains (S11, S13 and S20) the lowest growth rate (Figure 3J) in the same experiment. In

**Table 1:** Lowest (LGR) and highest growth rates (HGR) for Arctic strains of *Rhodomonas marina* that were grown at temperatures ranging between 1.4 and 15.9 °C.

Temperature (°C)	LGR ( $\text{day}^{-1}$ )	HGR ( $\text{day}^{-1}$ )	Percentage difference (%)
1.4 ± 0.1	0.18 ± 0.02 [S8 and S11]	0.22 ± 0.0 [S12]	20.0
3.8 ± 0.1	0.1 ± 0.02 [S11]	0.32 ± 0.0 [S12]	104.8
6.7 ± 0.2	0.23 ± 0.01 [S11]	0.46 ± 0.0 [S12]	66.7
9.9 ± 0.2	0.32 ± 0.01 [S8]	0.49 ± 0.03 [S13]	42.0
13.7 ± 0.1	0.46 ± 0.04 [S20]	0.99 ± 0.09 [S18]	73.1
15.9 ± 0.3	0.35 ± 0.02 [S20]	0.78 [S18]	76.1

Strain names for LGR and HGR are given in square brackets. The percentage differences between the lowest and highest values are also shown.

experiments with salinities 5 (Figure 3H) and 15 (Figure 3I) six out of seven strains had non-significantly different growth rates. Comparing growth rates for all seven strains examined at each of the three salinities tested, significant differences were found between 5 and 31 ( $p = 0.0004$ ) and 15 and 31 ( $p = 0.0119$ ) but not between 5 and 15 ( $p > 0.05$ ).

Comparing the strains individually (Figure 3A–G) three of them (S8, S11 and S13) grew equally well at the salinities tested (Figure 3A, B and D). For strain K-0435 and to some extent strains S12 and S20 these grew significantly faster with increasing salinities (Figure 3C, F and G, respectively). One strain (S18) had significantly lower growth rate at a salinity of 15 compared to growth rates at salinities 5 and 31 (Figure 3E).

## 4 Discussion and conclusion

The phylogenetic tree (Figure 1) based on a fast-evolving DNA fragment revealed a highly supported monophyletic clade for strains identified as *R. marina* (including *R. cf. baltica*). As expected for highly similar sequences (>99.6 %) noticeably short branch lengths among the strains of *R. marina* were noted irrespective of their geographic separation. The seven strains examined were therefore conspecific and likely represent the same population. It was noted that strain K-0332 identified as *R. cf. baltica*, clustered with K-0435 and the six Arctic strains. K-0332 was originally collected at the same location as K-0435 and the identification was based on light microscopy only. Identifications of cryptophytes are notoriously difficult when solely using morphological features available from light microscopical observations (e.g., Daugbjerg and Devantier 2024; Novarino 2012). In a recent study that included a phylogenetic inference based on nuclear-encoded SSU rDNA, *R. baltica* (strain

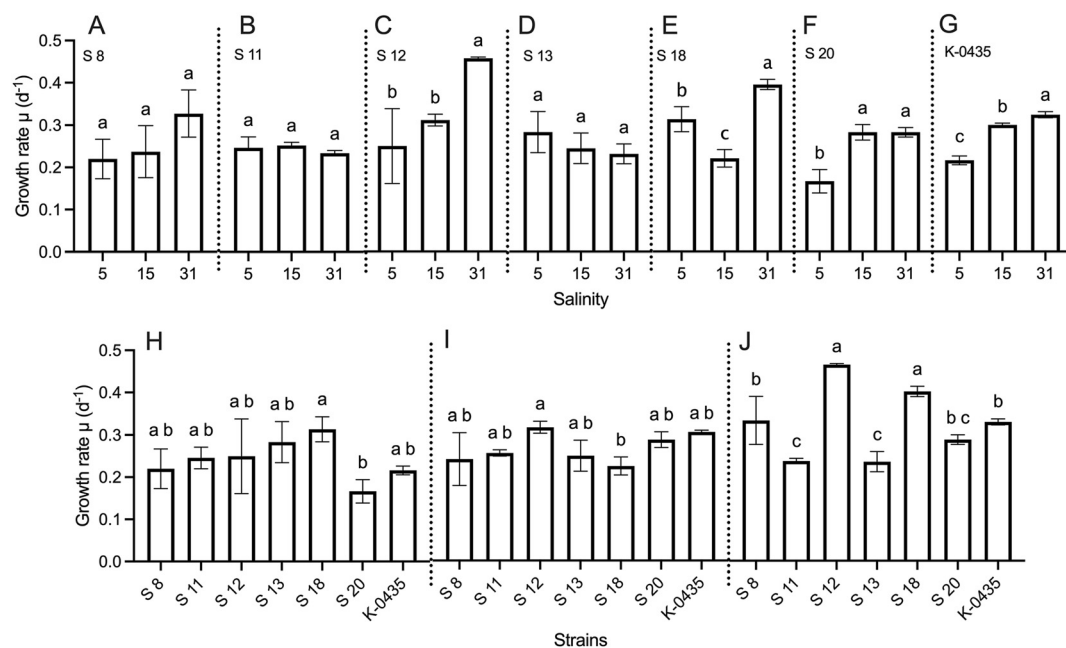


**Figure 3:** Growth rates ( $\mu \text{ day}^{-1}$ ) as a function of salinities (treatments at 5, 15 and 31) for seven strains of *Rhodomonas marina*. All autecological experiments were conducted as batch cultures at a temperature of 6.6 (salinity 5 and 15) or 6.7 °C (salinity 31). (A–G) Growth rates sorted by strain numbers. (H–J) Growth rates sorted by salinities. Identical lower-case letters show non-significant differences based on Tukey (HSD) post hoc tests.

**Table 2:** Lowest (LGR) and highest growth rates (HGR) for all seven strains of *Rhodomonas marina* that were grown at salinities 5, 15 and 31.

Salinity	LGR ( $\text{day}^{-1}$ )	HGR ( $\text{day}^{-1}$ )	Percentage difference (%)
5	0.16 ± 0.03 [S20]	0.3 ± 0.03 [S18]	60.9
15	0.22 ± 0.02 [S18]	0.31 ± 0.01 [S12]	34.0
31	0.23 ± 0.01 [S11]	0.46 ± 0.0 [S12]	66.7

Strain names for LGR and HGR are given in square brackets. The percentage differences between lowest and highest values are also shown.

NIES 700) and *R. marina* did not cluster together (Daugbjerg and Devantier 2024). The identity of K-0332 should therefore be reevaluated. In the study by Daugbjerg and Devantier (2024) one of the Arctic strains (S18) was characterized using a multifaceted approach and compared with phenotypically similar marine species of *Rhodomonas* including the original description of *R. marina*. This analysis led to the conclusion that S18 was identical to *R. marina* as originally described by Dangeard (1892) but as *Cryptomonas marina*. See Daugbjerg and Devantier (2024) for a historical account of the taxonomy of *R. marina*. Due to the high sequence similarity between S18, the other Arctic S-strains and K-0435 (>99.6 %) we conclude that they all represent *R. marina*. Thus, they could all form part of an autecological study elucidating intraspecific variation in response to the two abiotic variables.

The treatment of six Arctic strains isolated from the same water sample to different temperatures revealed a markedly dissimilar growth tolerance profile and thus the existence of intraspecific variation. Hence, for each temperature treatment multiple significant differences in growth rates were noted (Figure 2H–O). Two strains (S12 and S18) seemed generally better adapted for growing at the lowest temperatures (1.4–6.7 °C) while others (S8 and S11) did not appear to be well adapted to cold waters. Rather the latter two strains grew equally well as the other Arctic strains at mid-range temperatures (13.7–15.9 °C). One Arctic strain grew at a much warmer temperature of 20.1 °C. As only one Arctic strain was examined it is unknown if any of the other strains would also have grown at this temperature, which they otherwise would never have experienced in Arctic waters. In general, the six Arctic strains examined revealed optimum growth at temperatures which were approximately twice as high as the SST measured in July 2018 (5 °C) when the sample containing the isolates of *R. marina* was collected.

The strain from temperate waters (K-0435) did remarkably well over the temperature range provided (1.4–23.2 °C). Therefore, both the Arctic and this strain represent eurythermal organisms, thriving across a broad range of temperatures. Yet the growth rate did decrease from the second highest to the highest temperature treatment (Figure 2G).

Considering that the water temperature for most of the year is above 5 °C in Kattegat, where the strain was isolated from, it was somewhat unexpected that it grew also at the lower temperatures and in fact equally well to some of the Arctic strains (Figure 2H and I). The water temperature at the time of collecting the water sample containing *R. marina* was 7–8 °C (Richardson and Olsen 1992). An explanation for the wide temperature tolerance of the temperate strain may be that it can be found throughout the year in inner Danish waters (Hill et al. 1992) and therefore has adapted to higher temperature fluctuations than the Arctic strains. In Arctic waters the SST is less variable over a yearly cycle.

In another study using a similar autecological approach the Arctic marine cryptophyte *Baffinella frigidus* (Daugbjerg et al. 2018) revealed that growth stopped between 8 and 10 °C. Thus, *B. frigidus* represents a true Arctic cryptophyte better adapted to a cold-water marine environment. Based on the temperature experiments conducted here we hypothesize that *R. marina* was introduced to Disko Bay more recently from temperate waters perhaps by the north-going West Greenland Current. It is difficult to determine when it was first introduced to this marine environment. The impact of temperature on the growth rate of *Rhodomonas* has been studied multiple times, though typically with only single strains. A thorough comparison with the results obtained here was further complicated by the fact that many of the previously examined *Rhodomonas* strains were not identified to species but listed as *Rhodomonas* sp. (e.g., Chaloub et al. 2015; da Silva et al. 2009; De la Cruz et al. 2006; Latsos et al. 2020, 2021; Renaud et al. 2002). Furthermore, culture conditions differed (e.g., type of media, light levels). We need to keep these differences in mind when comparing maximum growth rates with other studies. In the present study the highest average growth rate for *R. marina* was 0.99 d<sup>-1</sup> at a temperature of 13.7 °C and a salinity of 31. This is similar to growth rates obtained in two other studies as De la Cruz et al. (2006) found a growth rate of 0.97 d<sup>-1</sup> at 20 °C and Chaloub et al. (2015) a growth rate of 1.15 d<sup>-1</sup> also at 20 °C for their isolates of *Rhodomonas* sp. Lower growth rates have also been reported as Renaud et al. (2002) estimated 0.35 d<sup>-1</sup> as the highest rate for their *Rhodomonas* sp. at a temperature of ca. 25 °C and da Silva et al. (2009) 0.68 d<sup>-1</sup> at 21 °C. Equally, these growth rates are similar to other results obtained during the temperature treatments of this study (Figure 2). Bartual et al. (2002) found growth rates ranging from 0.8 to 1.2 d<sup>-1</sup> when growing *R. salina* at a temperature of 19 °C while Hammer et al. (2002) reported 0.17 d<sup>-1</sup> at 15 °C and 0.25 d<sup>-1</sup> at 20 °C for their isolates. As expected, both intra- and interspecific variation exist with respect to maximum growth rates and studies conducted at higher temperatures did not always result in higher growth rates. This may show

unique biogeographical distributions and acclimation to marine habitats with different temperature regimes (Arctic to tropical waters). This information is important to the aquaculture industry when selecting strains of *Rhodomonas* for production of crustaceans (copepods) and bivalves. The results may also be of interest to biomedical and pharmaceutical industries focusing on natural products and their applications as we showed that the growth rate for one of the Arctic strains grown at ca. 14 °C was similar to those grown at 20 °C reported in the literature. However, future studies will need to determine how the concentrations and ratios of polyunsaturated fatty acids such as docosahexaenoic acid and eicosapentaenoic acid vary when grown at lower temperatures given their nutritional value (Oostlander et al. 2020).

The one-parameter experiments showed that salinity had less impact on growth rates of *R. marina* compared to temperature ( $p = 0.0011$ –0.2944). Despite some statistical differences (Figure 3A–G) all strains responded typically for euryhaline organisms in being able to grow under a wide range of salinities (Brand 1984). During the growth season, the Arctic strains have been exposed to variations in salinity levels ranging from low surface water concentrations near river outlets to full oceanic seawater further away from land and in deeper parts of the photic zone. Such seasonal variation may result in Arctic phytoplankton having adapted to changing osmotic pressures. As shown by Daugbjerg and Devantier (2024) an anterior contractile vacuole in *R. marina* likely also helps to keep an osmotic balance. Overall, the salinity results found in this study are in accordance with those of another Arctic cryptophyte *B. frigidus*, which also grew over a salinity range of 5–30 (Daugbjerg et al. 2018).

Contrary to the Arctic strains of *R. marina*, the growth rate of the Danish strain (K-0435) decreased significantly with lowering of the salinity ( $p < 0.0011$ ) (Figure 3G). Yet it had a growth performance equal to the Arctic strains (Figure 3H–J) and thus behaved as an estuarine species (Brand 1984). Interestingly, this strain has been cultured for over 30 years in L1 media with a salinity of ca. 30 and still can acclimate to a markedly lower salinity within just a few days. This clearly demonstrates the euryhaline nature of *R. marina*. It should also be noted that the salinity of the habitat where K-0435 was originally isolated from never falls below 14 (Richardson and Olsen 1992).

The highest average growth rate was found at a salinity of 31. This is similar to results obtained by Jepsen et al. (2019) when they reported an optimum growth rate for *R. salina* at a salinity of 29. Jepsen et al. (2019) also showed that *R. salina* (strain K-1487) could grow in salinities ranging from 5 to 65. The lower and upper lethal salinities for the strains of *R. marina* examined here were not determined.

To better evaluate the physiological acclimation capacity of phytoplankton populations to environmental variables, studies based on multiple clonal strains are needed. In general, such data can also be used for better model projections of the consequences of climate change. The current study has underlined the importance of this as growth rates differed by up to 105 % for the same genetically identical species (with 7 isolates tested) grown at different temperatures. Different growth rates were also obtained for strains grown at different salinities but with less variation compared to the temperature treatments. Clearly such phenotypic plasticity would remain undetected if only one strain was examined, and the growth performance would be either under- or over-estimated. However, the expected increase in global SST (Ruelaa et al. 2020) and decrease in ocean salinity (Llovel et al. 2019), compounding effects of climate change, did not seriously affect the growth potential of *R. marina*. This nanoflagellate is likely to thrive well under future temperature and salinity regimes. Other factors though, must also be considered (e.g., ocean acidification and nutrient availability) before understanding possible changes in the population structure of the cryptophyte *R. marina*.

Albeit interesting, changes in the profile and concentration of valuable biochemical compounds in *R. marina* due to variation in temperature and salinity treatments must await future studies. Here we have explored which of seven strains of *R. marina* had the best growth performance under different temperatures and salinities and therefore of interest for detailed biochemical characterization. Regarding the expected results of the autecological study, Experiment 1 proved that the highest growth performance occurred not at temperatures similar to the natural environment, but rather at elevated temperatures. The expected results of Experiment 2 aligned closely with the expected findings for Arctic phytoplankton, showing growth across a broad range of salinity levels.

**Research ethics:** Not applicable.

**Informed consent:** Not applicable.

**Author contributions:** C.B. Devantier: methodology, formal analyses, investigation, data curation, writing – original draft preparation. N. Daugbjerg: conceptualization, methodology, software, formal analyses, data curation, resources, investigation, visualization, writing – review & editing, supervision, project administration, funding acquisition. All authors have accepted responsibility for the entire content of this manuscript and approved its submission.

**Use of Large Language Models, AI and Machine Learning Tools:** None declared.

**Conflict of interest:** All authors state no conflict of interest.

**Research funding:** The Carlsberg Foundation provided equipment grants (grant numbers: 2013\_01\_0259 and CF14-0100).

**Data availability:** All data generated or analyzed during this study are included in this published article (and its Supplementary Material). DNA sequences of the internal transcribed spacer regions 1 and 2 of the seven strains of *Rhodomonas marina* determined have been deposited in GenBank and given accession numbers PX232446- PX232452.

## References

Abidizadegan, M., Peltomaa, E., and Blomster, J. (2021). The potential of cryptophyte algae in biomedical and pharmaceutical applications. *Front. Pharmcol.* 11: 618836.

Barton, A.D., Irwin, A.J., Finkel, Z.V., and Stock, C.A. (2016). Anthropogenic climate change drives shift and shuffle in North Atlantic phytoplankton communities. *Proc. Natl. Acad. Sci. U. S. A.* 113: 2964–2969.

Bartual, A., Lubián, L.M., Gálvez, J., and Niell, F. (2002). Effect of irradiance on growth, photosynthesis, pigment content and nutrient consumption in dense cultures of *Rhodomonas salina* (Wislouch) (Cryptophyceae). *Cienc. Mar.* 28: 381–392.

Beaugrand, G., Edwards, M., and Legendre, L. (2010). Marine biodiversity, ecosystem functioning, and carbon cycles. *Proc. Natl. Acad. Sci. U. S. A.* 107: 10120–10124.

Beaugrand, G., Edwards, M., Raybaud, V., Goberville, E., and Kirby, R.R. (2015). Future vulnerability of marine biodiversity compared with contemporary and past changes. *Nat. Clim. Change* 5: 695–701.

Behrenfeld, M.J., O’Malley, R.T., Siegel, D.A., McClain, C.R., Sarmiento, J.L., Feldman, G.C., Boss, E.S., Falkowski, P.G., and Letelier, R.M. (2006). Climate-driven trends in contemporary ocean productivity. *Nature* 444: 752–755.

Binzer, S.B., Svenssen, D.K., Daugbjerg, N., Alves-de-Souza, C., Pintoe, E., Hansen, P.J., Larsen, T.O., and Varga, E. (2019). A-B- and C-type prymnesins are clade specific compounds and chemotaxonomic markers in *Prymnesium parvum*. *Harmful Algae* 81: 10–17.

Bopp, L., Aumont, O., Cadule, P., Alvain, S., and Gehlen, M. (2005). Response of diatoms distribution to global warming and potential implications: a global model study. *Geophys. Res. Lett.* 32: L19606.

Brand, L.E. (1984). The salinity tolerance of forty-six marine phytoplankton isolates. *Estuar. Coast. Shelf Sci.* 18: 543–556.

Chaloub, R.M., Motta, N.M.S., de Araujo, S.P., de Aguiar, P.F., and da Silva, A.F. (2015). Combined effects of irradiance, temperature and nitrate concentration on phycoerythrin content in the microalga *Rhodomonas* sp. (Cryptophyceae). *Algal Res.* 8: 89–894.

Comeau, A.M., Li, W.K., Tremblay, J.E., Carmack, E.C., and Lovejoy, C. (2011). Arctic Ocean microbial community structure before and after the 2007 record sea ice minimum. *PLoS One* 6: e27492.

De la Cruz, F.L., Valenzuela-Espinoza, E., Millán-Núñez, R., Trees, C.C., Santamaría-del-Ángel, E., and Núñez-Cebriño, F. (2006). Nutrient uptake, chlorophyll *a* and carbon fixation by *Rhodomonas* sp. (Cryptophyceae) cultured at different irradiance and nutrient concentrations. *Aquacult. Eng.* 35: 51–60.

da Silva, A.F., Lourenço, S.O., and Chaloub, R.M. (2009). Effects of nitrogen starvation on the photosynthetic physiology of a tropical marine microalga *Rhodomonas* sp. (Cryptophyceae). *Aquat. Bot.* 91: 291–297.

Darriba, D., Taboada, G.L., Doallo, R., and Posada, D. (2012). jModelTest 2: more models, new heuristics and parallel computing. *Nat. Methods* 9: 772.

Daufresne, M., Lengfellner, K., and Sommer, U. (2009). Global warming benefits the small aquatic ecosystems. *Proc. Natl. Acad. Sci. U. S. A.* 106: 12788–12793.

Daugbjerg, N. and Devantier, C.B. (2024). Emendation of *Rhodomonas marina* (Cryptophyceae): insights from morphology, molecular phylogeny and water-soluble pigment in an arctic isolate. *Algae* 39: 75–96.

Daugbjerg, N., Lara, C., Gai, F.F., and Lovejoy, C. (2024). *Plocaisiomonas psychrophila* gen. et sp. nov. (Pelagophyceae, Heterokontophyta), an Arctic marine nanoflagellate characterized by microscopy, pigments and molecular phylogeny. *Eur. J. Phycol.* 59: 362–378.

Daugbjerg, N., Norlin, A., and Lovejoy, C. (2018). *Baffinella frigidus* gen. et sp. nov. (Baffinellaceae fam. nov., Cryptophyceae) from Baffin Bay: morphology, pigment profile, phylogeny, and growth rate response to three abiotic factors. *J. Phycol.* 54: 665–680.

Edwards, M. and Richardson, A.J. (2004). Impact of climate change on marine pelagic phenology and trophic mismatch. *Nature* 430: 881–884.

Guillard, R. and Hargraves, P. (1993). *Stichochrysis immobilis* is a diatom, not a chrysophyte. *Phycologia* 32: 234–236.

Guinder, V. and Molinero, J. (2013). Climate change effects on marine phytoplankton. In: Arias, A.H., and Menendez, M.C. (Eds.). *Marine ecology in a changing world*. CRC Press, Boca Raton, pp. 68–90.

Guindon, S., Dufayard, J.F., Lefort, V., Anisimova, M., Hordijk, W., and Gascuel, O. (2010). New algorithms and methods to estimate maximum-likelihood phylogenies: assessing the performance of PhyML 3.0. *Syst. Biol.* 59: 307–321.

Hammer, A., Schumann, R., and Schubert, H. (2002). Light and temperature acclimation of *Rhodomonas salina* (Cryptophyceae): photosynthetic performance. *Aquat. Microb. Ecol.* 29: 287–296.

Henson, S.A., Cael, B.B., Allen, S.R., and Dutkiewicz, S. (2021). Future phytoplankton diversity in a changing climate. *Nat. Commun.* 12: 5372.

Hill, D., Moestrup, Ø., and Vørs, N. (1992). Rekylalger (Cryptophyceae). In: Thomsen, H.A. (Ed.). *Plankton i de indre danske farvande*. Hafvorskning fra Miljøstyrelsen, Copenhagen, pp. 251–265.

Jepsen, P.M., Thoisen, C.V., Carron-Cabaret, T., Pinyol-Galleñí, A., Nielsen, S.L., and Hansen, B.W. (2019). Effects of salinity, commercial salts, and water type on cultivation of the cryptophyte microalgae *Rhodomonas salina* and the calanoid copepod *Acartia tonsa*. *J. World Aquacult. Soc.* 50: 104–118.

Käse, L. and Geuer, J.K. (2018). Phytoplankton responses to marine climate change—an introduction. In: Jungblut, S., Liebich, V., and Bode, M. (Eds.). *YOUNMARES 8—Oceans across Boundaries: learning from each other*, pp. 55–71.

Kremp, A., Godhe, A., Egardt, J., Dupont, S., Suikkanen, S., Casabianca, S., and Penna, A. (2012). Intraspecific variability in the response of bloom-forming marine microalgae to changed climate conditions. *Ecol. Evol.* 2: 1195–1207.

Latsos, C., van Houcke, J., Blommaert, L., Verbeeke, G.P., Kromkamp, J., and Timmermans, K.R. (2021). Effect of light quality and quantity on productivity and phycoerythrin concentration in the cryptophyte *Rhodomonas* sp. *J. Appl. Phycol.* 33: 729–741.

Latsos, C., van Houcke, J., and Timmermans, K.R. (2020). The effect of nitrogen starvation on biomass yield and biochemical constituents of *Rhodomonas* sp. *Front. Mar. Sci.* 7: 563333.

LeGresley, M. and McDermott, G. (2010). Counting chamber methods for quantitative phytoplankton analysis - haemocytometer, Palmer- Maloney cell and Sedgewick-Rafter cell. In: Karlson, B., Cusack, C., and Bresnan, E. (Eds.). *Intergovernmental Oceanographic Commission of UNESCO. 2010. Microscopic and molecular methods for quantitative phytoplankton analysis*. UNESCO. IOC Manuals and Guides. 55 (IOC/2010/MG/55), Paris, pp. 25–27.

Li, W.K.W., McLaughlin, F.A., Lovejoy, C., and Carmack, E.C. (2009). Smallest algae thrive as the Arctic Ocean freshens. *Science* 326: 539.

Llovel, W., Purkey, S., Meyssignac, B., Blazquez, A., Kolodziejczyk, N., and Bamber, J.L. (2019). Global ocean freshening, ocean mass increase and global mean sea level rise over 2005–2015. *Sci. Rep.* 9: 17717.

Novarino, G. (2012). Cryptomonad taxonomy in the 21st century: the first two hundred years. In: Wolowski, K., Kaczmarśka, I., Ehrman, J.E., and Wojtka, A.Z. (Eds.). *Phycological reports: current advances in algal taxonomy and its applications. Phylogenetic, ecological and applied perspective*. Institute of Botany Polish Academy of Sciences, Krakow, pp. 19–52.

Oostlander, P.C., van Houcke, J., Wijffels, R.H., and Barbosa, M.J. (2020). Optimization of *Rhodomonas* sp. under continuous cultivation for industrial applications in aquaculture. *Algal Res.* 47: 101889.

Pančić, M., Hansen, P.J., Tammilehto, A., and Lundholm, N. (2015). Resilience to temperature and pH changes in a future climate change scenario in six strains of the polar diatom *Fragilariaopsis cylindrus*. *Biogeosciences* 12: 4235–4244.

Pascher, A. (Ed.) (1913). *Die Süßwasserflora Deutschlands, Österreichs und der Schweiz*. G. Fischer, Jena, pp. 96–114.

Peltomaa, E., Johnson, M.A., and Taipale, S.J. (2018). Marine cryptophytes are great sources of EPA and DHA. *Mar. Drugs* 16: 3.

Renaud, S.M., Thinh, L.V., Lambrinidis, G., and Parry, D.L. (2002). Effect of temperature on growth, chemical composition and fatty acid composition of tropical Australian microalgae grown in batch cultures. *Aquaculture* 211: 195–214.

Richardson, K. and Olsen, V.O. (1992). Hydrografiske- og kemiske målinger. In: Fenchel, T. (Ed.). *Planktonodynamik af stofomsætning i Kattegat*. Havforskning fra Miljøstyrelsen no 10. Miljøministeriet, København, pp. 19–29.

Rizwan, M., Mujtaba, G., Memon, S.A., Lee, K., and Rashid, N. (2018). Exploring the potential of microalgae for new biotechnology applications and beyond: a review. *Renew. Sustain. Energy Rev.* 92: 394–404.

Ronquist, F. and Huelsenbeck, J.P. (2003). MrBayes 3: Bayesian phylogenetic inference under mixed models. *Bioinformatics* 19: 1572–1574.

Ruelaa, R., Sousaa, M.C., deCastrob, M., and Diasa, J.M. (2020). Global and regional evolution of sea surface temperature under climate change. *Global Planet Change* 190: 103190.

Salles, S. and Mercado, J.M. (2020). Chapter 24. Biodiversity distribution patterns of marine phytoplankton and their main threats (climate change, eutrophication and acidification). In: Kim, S.-K. (Ed.). *Encyclopedia of marine biotechnology*. John Wiley & Sons Ltd, Chichester, UK, pp. 661–679.

Stocker, T.F., Dahe, Q., Plattner, G.-K., Alexander, L.V., Allen, S.K., Bindoff, N.L., Bréon, F.-M., Church, J.A., Cubasch, U., Emori, S., et al. (2013). Technical summary. In: Stocker, T.F., Dahe, Q., Plattner, G.-K., Tignor, M., Allen, S.K., Boschung, J., Nauels, A., Xia, Y., Bex, V., and Midgley, P.M. (Eds.). *Climate change 2013: the physical science basis. Contribution of working group I to the fifth assessment Report of the intergovernmental Panel on climate change*. Cambridge University Press, Cambridge, UK and New York, NY, USA.

IPCC (2023). SectionsTeam, Core Writing, Lee, H., and Romero, J. (Eds.). *Climate change 2023: synthesis report. Contribution of working groups I, II and III to the sixth assessment report of the intergovernmental panel on climate change*. IPCC, Geneva, Switzerland, pp. 35–115.

Thomalla, S.J., Nicholson, S.A., Ryan-Keogh, T.J., and Smith, M.E. (2023). Widespread changes in Southern Ocean phytoplankton blooms linked to climate drivers. *Nat. Clim. Chang.* 13: 975–984.

Vilchis, M.C.L. (2022). Cryptophyte: biology, culture, and biotechnological applications. In: Zepka, L.Q., Jacob-Lopes, E., and Deprá, M. (Eds.). *Progress in microalgae research: a path for shaping sustainable futures*. IntechOpen, London, UK, pp. 17–40.

Vu, M.T.T., Douëtte, C., Rayner, T.A., Thoisen, C., Nielsen, S.L., and Hansen, B.W. (2016). Optimization of photosynthesis, growth, and biochemical composition of the microalga *Rhodomonas salina*: an established diet for live feed copepods in aquaculture. *J. Appl. Phycol.* 28: 1485–1500.

White, T.J., Bruns, T., Lee, S., and Taylor, J. (1990). Amplification and direct sequencing of fungal ribosomal RNA genes for phylogenetics. In: Innis, M.A., Gelfand, D.H., Sninsky, J.J., and White, T.J. (Eds.). *PCR protocols: a guide to methods and applications*. Academic Press, New York, USA, pp. 315–322.

Winder, M., Berger, S.A., Lewandowska, A., Aberle, N., Lengfellner, K., Sommer, U., and Diehl, S. (2012). Spring phenological responses of marine and freshwater plankton to changing temperature and light conditions. *Mar. Biol.* 159: 2491–2501.

Winder, M. and Sommer, U. (2012). Phytoplankton response to a changing climate. *Hydrobiologia* 698: 5–16.

Wood, A.M., Everroad, R., and Wingard, L. (2005). Measuring growth rates in microalgal cultures. In: Anderson, R. (Ed.). *Algal culturing techniques*. Elsevier Academic Press, pp. 269–288.

Yamaguchi, R., Rodgers, K.B., Timmermann, A., Stein, K., Schlunegger, S., Bianchi, D., Dunne, J.P., and Slater, R.D. (2022). Trophic level decoupling drives future changes in phytoplankton bloom phenology. *Nat. Clim. Chang.* 12: 469–476.

---

**Supplementary Material:** This article contains supplementary material (<https://doi.org/10.1515/bot-2024-0080>).